

Vibrational imaging of newly synthesized proteins in live cells by stimulated Raman scattering microscopy

Lu Wei^a, Yong Yu^{b,c}, Yihui Shen^a, Meng C. Wang^{b,c,1}, and Wei Min^{a,d,1}

^aDepartment of Chemistry and ^dKavli Institute for Brain Science, Columbia University, New York, NY 10027; and ^bDepartment of Molecular and Human Genetics and ^cHuffington Center on Aging, Baylor College of Medicine, Houston, TX 77030

Edited by David A. Tirrell, California Institute of Technology, Pasadena, CA, and approved May 31, 2013 (received for review February 27, 2013)

Synthesis of new proteins, a key step in the central dogma of molecular biology, has been a major biological process by which cells respond rapidly to environmental cues in both physiological and pathological conditions. However, the selective visualization of a newly synthesized proteome in living systems with subcellular resolution has proven to be rather challenging, despite the extensive efforts along the lines of fluorescence staining, autoradiography, and mass spectrometry. Herein, we report an imaging technique to visualize nascent proteins by harnessing the emerging stimulated Raman scattering (SRS) microscopy coupled with metabolic incorporation of deuterium-labeled amino acids. As a first demonstration, we imaged newly synthesized proteins in live mammalian cells with high spatial-temporal resolution without fixation or staining. Subcellular compartments with fast protein turnover in HeLa and HEK293T cells, and newly grown neurites in differentiating neuron-like N2A cells, are clearly identified via this imaging technique. Technically, incorporation of deuterium-labeled amino acids is minimally perturbative to live cells, whereas SRS imaging of exogenous carbon-deuterium bonds (C–D) in the cell-silent Raman region is highly sensitive, specific, and compatible with living systems. Moreover, coupled with label-free SRS imaging of the total proteome, our method can readily generate spatial maps of the quantitative ratio between new and total proteomes. Thus, this technique of nonlinear vibrational imaging of stable isotope incorporation will be a valuable tool to advance our understanding of the complex spatial and temporal dynamics of newly synthesized proteome in vivo.

stable isotope labeling | stimulated Raman microscopy | protein synthesis

The proteome of a cell is highly dynamic in nature and tightly regulated by both protein synthesis and degradation to actively maintain homeostasis. Many intricate biological processes, such as cell growth, differentiation, diseases, and response to environmental stimuli, require protein synthesis and translational control (1). In particular, long-lasting forms of synaptic plasticity, such as those underlying long-term memory, require new protein synthesis in a space- and time-dependent manner (2–4). Therefore, direct visualization and quantification of newly synthesized proteins at a global level are indispensable to unraveling the spatial-temporal characteristics of the proteomes in live cells.

Extensive efforts have been devoted to probing protein synthesis via fluorescence contrast. The inherent fluorescence of green fluorescent protein (GFP) and its genetic encodability allow one to follow a given protein of interest inside living cells with high spatial and temporal resolution (5, 6). However, GFP tagging through genetic manipulation works only on individual proteins but not at the whole-proteome level. To probe newly synthesized proteins at the proteome level, a powerful technique named bioorthogonal noncanonical amino acid tagging (BONCAT) was developed by metabolic incorporation of unnatural amino acids containing reactive chemical groups such as azide or alkyne (7–13). A related labeling method was recently demonstrated using an alkyne analog of puromycin (14). Newly synthesized proteins can then be visualized through subsequent conjugation of the reactive amino acids to fluorescent tags via click chemistry (15). Unfortunately, these fluorescence-based methods

generally require nonphysiological fixation and subsequent dye staining and washing.

In addition to fluorescence tagging, radioisotope or stable isotope labeling is another powerful tool to trace and quantify proteome dynamics. Classical radioisotope-labeled amino acids (e.g., [³⁵S]methionine) provide vigorous analysis of global protein synthesis. However, samples must be fixed and then exposed to film for autoradiography. For stable isotopes, the discovery of deuterium by Urey in 1932 immediately led to the pioneer work of Schoenheimer and Rittenberg studying intermediary metabolism (16, 17). To study proteome changes between different cells or under different conditions, stable isotope labeling by amino acids in cell culture (SILAC) coupled with mass spectrometry (MS) has matured into a popular method for quantitative proteomics (18–21). However, SILAC-MS does not usually provide spatial information down to subcellular level and its invasive nature also limits its application for live-cell imaging. The same limitation applies to the recent ribosome profiling study using deep sequencing technique (22).

Therefore, it is highly challenging and desirable to be able to quantitatively image proteome synthesis in live cells with high spatial-temporal resolution. Herein, we report using stimulated Raman scattering (SRS) microscopy, an emerging vibrational imaging technique, for the visualization of nascent proteins in live cells coupled through metabolic incorporation of deuterium-labeled amino acids (Fig. 1). Newly synthesized proteins are imaged via their unique vibrational signature of carbon-deuterium bonds (C–D). Vibrational imaging by Raman contrast is a rapidly growing field. Spontaneous Raman microscopy can offer spatially resolved chemical information based on the vibration frequencies of characteristic chemical bonds. However, spontaneous Raman scattering is an intrinsically weak process, hence not ideal for fast live-cell imaging (23). As a nonlinear technique, coherent anti-Stokes Raman scattering (CARS) offers much higher imaging speed by virtue of coherent amplification (24–28). Unfortunately, CARS suffers from spectral distortion, unwanted nonresonant background, nonstraightforward concentration dependence, and coherent image artifact (25). Most recently, SRS microscopy has emerged to supersede CARS microscopy in almost all aspects (29–38). Using Einstein's stimulated emission principle (39, 40), SRS has achieved unprecedented sensitivity down to ~1,000 retinoic acid molecules and up to video rate imaging speed in vivo (30, 33). Unlike CARS, SRS microscopy exhibits straightforward image interpretation and quantification without complications from the nonresonant background and phase-matching conditions (41, 42). Consequently, not only is the signal-to-noise ratio improved over CARS, but the Raman spectral fidelity is

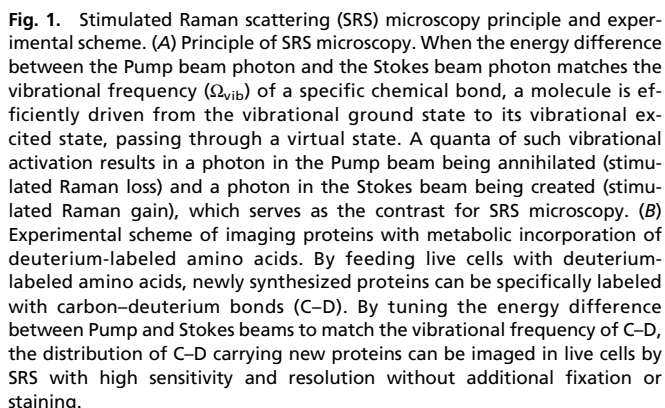
Author contributions: L.W., M.C.W., and W.M. designed research; L.W., Y.Y., and Y.S. performed research; L.W. analyzed data; and L.W., Y.Y., Y.S., M.C.W., and W.M. wrote the paper.

Conflict of interest statement: Columbia University has filed a patent application based on this work.

This article is a PNAS Direct Submission.

¹To whom correspondence may be addressed. E-mail: wm2256@columbia.edu or wmeng@bcm.edu.

This article contains supporting information online at www.pnas.org/lookup/suppl/doi:10.1073/pnas.1303768110/-DCSupplemental.



First, we demonstrated the proof-of-concept of our technique on live HeLa cells using a single deuterium-labeled essential amino acid, leucine- d_{10} . Then we optimized the incorporation efficiency of the deuterium isotope into nascent proteins and showed broad applicability of the method on several mammalian cell lines, particularly, its unique advantage in generating spatial maps of the quantitative ratio between new and old proteomes. Furthermore, besides visualizing newly synthesized proteins in cell bodies, the ability to image nascent proteins in neurites of neuron-like mouse neuroblastoma Neuro-2A (N2A) cells upon differentiation was also shown, demonstrating the prospect of studying *de novo* protein synthesis during neuronal plasticity, such as long-term memory.

Physical Principle of Isotope-Based SRS Imaging. SRS microscopy is a molecular-contrast, highly sensitive imaging technique with intrinsic 3D sectioning capability. It selectively images the distribution of molecules that carry a given type of chemical bonds through resonating with the specific vibrational frequency of the targeted bonds (30, 33, 41). As Fig. 1A illustrates, by focusing both temporally and spatially overlapped Pump and Stokes laser pulse trains into samples, the rate of vibrational transition is

Here, we detect the vibrational signal of C–D as an indicator for newly synthesized proteins that metabolically incorporate deuterium-labeled amino acids (Fig. 1B). When hydrogen atoms are replaced by deuterium, the chemical and biological activities of biomolecules remain largely unmodified. Intriguingly, the C–D stretching motion displays a distinct vibrational frequency from all of the other vibrations of biological molecules inside live cells. It is known from classical mechanics that the frequency of vibrational oscillation, Ω_{vib} , inversely scales with the square root of the reduced mass of the oscillator $\Omega_{\text{vib}} = (1/2\pi)\sqrt{k/\mu}$, where k is the spring constant of the corresponding chemical bond, and μ denotes the reduced mass of the oscillator. The reduced mass of the C–D oscillator is increased by two folds when hydrogen is replaced by deuterium. Based on the above equation, Ω_{vib} would be reduced by a factor of $\sqrt{2}$. Indeed, the experimentally measured stretching frequency is shifted from $\sim 2,950\text{ cm}^{-1}$ of C–H to $\sim 2,100\text{ cm}^{-1}$ of C–D. Remarkably, the vibrational frequency of $2,100\text{ cm}^{-1}$ is located in a cell-silent spectral window in which no other Raman peaks exist (Fig. S1), thus enabling detection of exogenous C–D with both high specificity and sensitivity.

Based on the above spectra, we choose to target the central $2,133\text{ cm}^{-1}$ vibrational peak of C–D to acquire SRS images of nascent proteins in live HeLa cells. As expected, HeLa cells growing in regular medium show no detectable SRS contrast at $2,133\text{ cm}^{-1}$ (Fig. 2C), which is consistent with the flat spectral baseline (red in Fig. 2B) in the cell-silent region. In contrast, SRS image of HeLa cells growing in the medium containing 0.8 mM

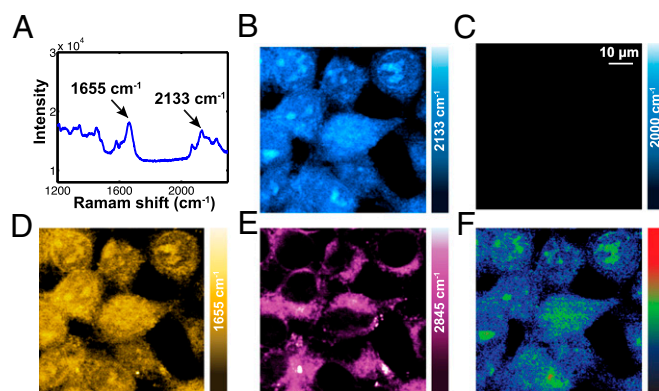


Fig. 5. SRS imaging of newly synthesized proteins by metabolic incorporation of a deuterium-labeled set of all amino acids in live human embryonic kidney (HEK293T) cells. (A) The spontaneous Raman spectrum of HEK293T cells incubated with a deuterium-labeled set of all amino acids for 12 h shows a $2,133\text{ cm}^{-1}$ C–D peak nearly as high as the amide I ($1,655\text{ cm}^{-1}$) peak. (B) SRS image targeting the central $2,133\text{ cm}^{-1}$ vibrational peak of C–D shows newly synthesized proteins in live HEK293T cells displaying a similar signal level as HeLa cells at 12 h (Fig. 4B). (C) As a comparison, the off-resonant image is still background free. (D and E) Multicolor SRS images of intrinsic cell molecules: total proteins [$1,655\text{ cm}^{-1}$ (D)] and lipids [$2,845\text{ cm}^{-1}$ (E)]. (F) The ratio image between new proteins ($2,133\text{ cm}^{-1}$) and total proteins ($1,655\text{ cm}^{-1}$) illustrates a spatial map for nascent protein distribution.

Conclusion

The ability to visualize newly synthesized proteomes in biological systems will greatly advance our understanding of complex cellular functions occurring in space and time (1–4). Currently, this endeavor is mainly pursued by several distinct contrast mechanisms including fluorescence staining, autoradiography, and mass spectroscopy. Here, we report a new technique of SRS microscopy coupled with stable isotope labeling (deuterium labeling in this study) to address this challenge. The major advantages of our technique lie in the following aspects. First, our approach is essentially noninvasive and completely compatible with the live-cell physiology. This is in contrast with earlier methods of autoradiography and BONCAT. In terms of sample preparations, the deuterium isotope has a high degree of similarity with the cells' endogenous counterpart (18–21). In terms of imaging conditions, SRS directly probes vibrational transitions in a stain-free manner using near-infrared lasers whose phototoxicity is low especially when using picosecond pulses. We note that a recent technique called multiisotope imaging mass spectrometry has also demonstrated a high-resolution isotope imaging ability (48, 49), but with a highly destructive nature due to the use of an ion microscope. Second, overcoming the major problems of CARS microscopy, SRS is an emerging nonlinear Raman microscopy with purely chemical contrast and high sensitivity, enabling fast imaging speed up to video rate in live animals and humans (41, 42). Our current electronics offers imaging speed of $\sim 26\text{ s}$ per frame (512×512 pixels), which could be accelerated to video rate using a custom lock-in amplifier (33). As a comparison, spontaneous Raman microscopy relies on a feeble signal, which is easily overwhelmed by cell autofluorescence and needs long integration time ($> \text{hours}$) for imaging (23), and is thus undesirable for live-cell imaging. In fact, spontaneous Raman microscopy has been applied for detection of newly synthesized proteins, but was only possible with fixed cells (50). Third, SRS microscopy can readily offer the intrinsic total proteins distribution in a label-free manner. Such a valuable internal reference of total proteins is very hard to obtain for techniques such as BONCAT or mass spectroscopy without destruction of the cells.

Therefore, we have demonstrated SRS microscopy coupled with deuterium-labeled amino acids incorporation as an imaging technique for visualization of newly synthesized proteins in living

mammalian cells under physiological conditions without any fixation or staining. From the perspective of biological applications, the biocompatibility of both deuterium labeling and SRS imaging renders this technique the prospect of revealing spatial–temporal proteome dynamics in more complex systems such as live animals. From the perspective of imaging technology, nonlinear vibrational microscopy is well suited for visualizing the metabolic incorporation of isotope labeled precursors of macromolecules for its high sensitivity, specificity, and the non-invasive nature. We expect this strategy to be generalized and expanded to other stable isotopes such as ^{13}C and ^{15}N .

Materials and Methods

SRS Microscopy. The experimental setup is shown in Fig. 1B. Spatially and temporally overlapped pulsed Pump (tunable from 720 to 990 nm, 7 ps, 80-MHz repetition rate) and Stokes ($1,064\text{ nm}$, 5–6 ps, 80-MHz repetition rate, modulated at 10 MHz) beams, which are provided by picoEMERALD from Applied Physics & Electronics are coupled into an inverted laser-scanning microscope (FV1000 MPE; Olympus) optimized for near-IR throughput. A 60 \times water objective (UPlanAPO/IR; 1.2 N.A.; Olympus) is used for all cell imaging. After passing through the sample, the forward going Pump and Stokes beams are collected in transmission by a high N.A. condenser and imaged onto a large area Si photodiode. A high OD bandpass filter (890/220, Chroma) is used to block the Stokes beam completely and to transmit the Pump beam only for the detection of the stimulated Raman loss signal. The output current from the photodiode is terminated, filtered, and demodulated by a lock-in amplifier (SR844; Stanford Research Systems) at 10 MHz to ensure shot noise-limited detection sensitivity. For imaging, 512×512 pixels are acquired for one frame (26 s per frame) with a 100- μs pixel dwell time and 20- μs time constant from the lock-in amplifier. Powers after 60 \times IR objective used for imaging are as follows: 61 mW for modulated Stokes beam; 145 mW for the Pump beam of $2,133\text{ cm}^{-1}$, $2,000\text{ cm}^{-1}$,

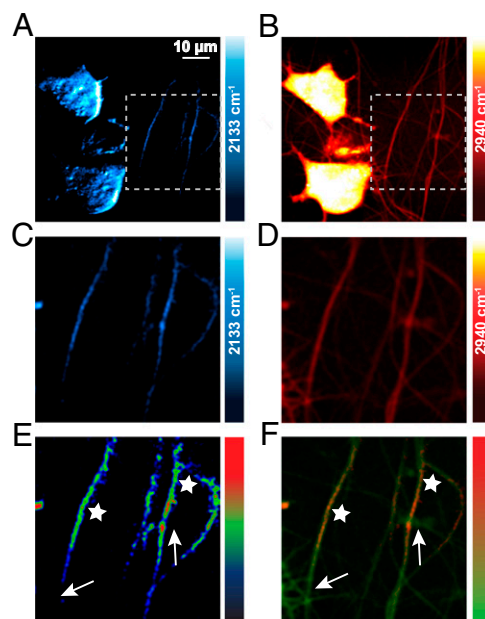


Fig. 6. SRS imaging of newly synthesized proteins in both cell bodies and newly grown neurites of neuron-like differentiable mouse neuroblastoma (N2A) cells. During the cell differentiation process by serum deprivation and $1\text{ }\mu\text{M}$ retinoic acid, deuterium-labeled all-amino acids medium is also supplied for 24 h. (A) SRS images targeting the $2,133\text{ cm}^{-1}$ peak of C–D show newly synthesized proteins. (B) SRS images targeting the $2,940\text{ cm}^{-1}$ CH_3 show total proteins. (C and D) Zoomed-in images as indicated in the white dashed squares in A and B. (E) Ratio image between new protein (C) and total proteins (D). Although the starred neurites show high percentage of new proteins, the arrows indicate neurites displaying very low new protein percentage. (F) Merged image between new protein (C) (red channel) and total proteins (D) (green channel). Similarly, the starred regions show obvious new proteins, whereas the arrows indicate regions that have undetectable new protein signal.

and 1,655 cm^{-1} channels; and 64 mW for Pump beam of 2,950 cm^{-1} and 2,845 cm^{-1} channels.

Metabolic Labeling of the Newly Synthesized Proteins by Deuterium-Labeled Amino Acids. Deuterium-labeled leucine- d_{10} medium is made by adding leucine- d_{10} (0.8 mM), lysine (0.8 mM), and arginine (0.4 mM) (Sigma) into leucine-, lysine-, and arginine-deficient DMEM (Sigma). Deuterium-labeled all-amino acids medium is made by adding uniformly deuterium-labeled amino acid mix (20 aa) (Cambridge Isotope) into leucine-, lysine-, and arginine-deficient DMEM (Sigma). The final concentration of leucine- d_{10} is adjusted to be 0.8 mM among the amino acid mix. (Because the starting medium is leucine, lysine, and arginine deficient, by adding the deuterium-labeled 20-aa mix, we essentially deuterate all of the leucine, lysine, and arginine as well as about one-half of the other amino acids.) Cells are seeded on a coverslip in a petri dish with 2 mL of regular DMEM with 10% (vol/vol) FBS and 1% penicillin/streptomycin (Invitrogen) for 20 h. The regular medium is then replaced with medium containing either leucine- d_{10} or a deuterium-labeled set of all amino acids. After incubation for a certain amount of

time, the coverslip is taken out to make an imaging chamber filled with PBS for SRS imaging. For N2A cells, in the process of induced cell differentiation with serum deprivation and 1 μM retinoic acid, the deuterium-labeled set of all amino acids is supplemented.

Spontaneous Raman Spectroscopy. The spontaneous Raman spectra were acquired using a laser Raman spectrometer (inVia Raman microscope; Renishaw) at room temperature. A 27-mW (after objective), 532-nm diode laser was used to excite the sample through a 50 \times , N.A. 0.75 objective (NPLAN EPI; Leica). The total data acquisition was performed during 80 s using the WiRE software.

ACKNOWLEDGMENTS. We thank F. Hu, Z. Chen, V. W. Cornish, D. Peterka, and R. Yuste for helpful discussion. We are grateful to S. Buffington, M. Costa-Mattioli, and M. Sakamoto for providing hippocampal neurons, and Y. Li for his assistance on the spontaneous Raman microscope. We acknowledge support from Ellison Medical Foundation fellowships (to M.C.W.) and National Institutes of Health Director's New Innovator Award (to W.M.).

- Hershey JWB, Sonenberg N, Mathews MB, eds (2012) *Protein Synthesis and Translational Control* (Cold Spring Harbor Lab Press, Cold Spring Harbor, NY).
- Martin KC, Barad M, Kandel ER (2000) Local protein synthesis and its role in synapse-specific plasticity. *Curr Opin Neurobiol* 10(5):587–592.
- Kandel ER (2001) The molecular biology of memory storage: A dialogue between genes and synapses. *Science* 294(5544):1030–1038.
- Ho VM, Lee JA, Martin KC (2011) The cell biology of synaptic plasticity. *Science* 334(6056):623–628.
- Chalfie M, Tu Y, Euskirchen G, Ward WW, Prasher DC (1994) Green fluorescent protein as a marker for gene expression. *Science* 263(5148):802–805.
- Tsien RY (1998) The green fluorescent protein. *Annu Rev Biochem* 67:509–544.
- Dieterich DC, Link AJ, Graumann J, Tirrell DA, Schuman EM (2006) Selective identification of newly synthesized proteins in mammalian cells using bioorthogonal noncanonical amino acid tagging (BONCAT). *Proc Natl Acad Sci USA* 103(25):9482–9487.
- Beatty KE, et al. (2006) Fluorescence visualization of newly synthesized proteins in mammalian cells. *Angew Chem Int Ed Engl* 45(44):7364–7367.
- Beatty KE, Tirrell DA (2008) Two-color labeling of temporally defined protein populations in mammalian cells. *Bioorg Med Chem Lett* 18(22):5995–5999.
- Roche FK, Marsick BM, Letourneau PC (2009) Protein synthesis in distal axons is not required for growth cone responses to guidance cues. *J Neurosci* 29(3):638–652.
- Dieterich DC, et al. (2010) In situ visualization and dynamics of newly synthesized proteins in rat hippocampal neurons. *Nat Neurosci* 13(7):897–905.
- Tcherkezian J, Brittis PA, Thomas F, Roux PP, Flanagan JG (2010) Transmembrane receptor DCC associates with protein synthesis machinery and regulates translation. *Cell* 141(4):632–644.
- Hinz FI, Dieterich DC, Tirrell DA, Schuman EM (2012) Non-canonical amino acid labeling in vivo to visualize and affinity purify newly synthesized proteins in larval zebrafish. *ACS Chem Neurosci* 3(1):40–49.
- Liu J, Xu Y, Stoleru D, Salic A (2012) Imaging protein synthesis in cells and tissues with an alkyne analog of puromycin. *Proc Natl Acad Sci USA* 109(2):413–418.
- Boyce M, Bertozzi CR (2011) Bringing chemistry to life. *Nat Methods* 8(8):638–642.
- Schoenheimer R, Rittenberg D (1935) Deuterium as an indicator in the study of intermediary metabolism. *J Biol Chem* 111(1):163–168.
- Schoenheimer R, Rittenberg D (1938) Application of isotopes to the study of intermediary metabolism. *Science* 87(2254):221–226.
- Ong SE, et al. (2002) Stable isotope labeling by amino acids in cell culture, SILAC, as a simple and accurate approach to expression proteomics. *Mol Cell Proteomics* 1(5):376–386.
- Mann M (2006) Functional and quantitative proteomics using SILAC. *Nat Rev Mol Cell Biol* 7(12):952–958.
- Harsha HC, Molina H, Pandey A (2008) Quantitative proteomics using stable isotope labeling with amino acids in cell culture. *Nat Protoc* 3(3):505–516.
- Geiger T, et al. (2011) Use of stable isotope labeling by amino acids in cell culture as a spike-in standard in quantitative proteomics. *Nat Protoc* 6(2):147–157.
- Ingolia NT, Lareau LF, Weissman JS (2011) Ribosome profiling of mouse embryonic stem cells reveals the complexity and dynamics of mammalian proteomes. *Cell* 147(4):789–802.
- Potma EO, Xie XS (2008) Theory of spontaneous and coherent Raman scattering. *Handbook of Biomedical Nonlinear Optical Microscopy*, eds Masters BR, So PTC (Oxford Univ Press, New York).
- Zumbusch A, Holtom GR, Xie XS (1999) Three-dimensional vibrational imaging by coherent anti-Stokes Raman scattering. *Phys Rev Lett* 82(20):4142–4145.
- Evans CL, Xie XS (2008) Coherent anti-stokes Raman scattering microscopy: Chemical imaging for biology and medicine. *Annu Rev Anal Chem (Palo Alto Calif)* 1:883–909.
- Cheng JX, Xie XS (2004) Coherent anti-Stokes Raman scattering microscopy: Instrumentation, theory, and applications. *J Phys Chem B* 108(3):827–840.
- Pezacki JP, et al. (2011) Chemical contrast for imaging living systems: Molecular vibrations drive CARS microscopy. *Nat Chem Biol* 7(3):137–145.
- Suhalim JL, Boik JC, Tromberg BJ, Potma EO (2012) The need for speed. *J Biophotonics* 5(5–6):387–395.
- Ploetz E, Laimgruber S, Berner S, Zinth W, Gilch P (2007) Femtosecond stimulated Raman microscopy. *Appl Phys B* 87(3):389–393.
- Freudiger CW, et al. (2008) Label-free biomedical imaging with high sensitivity by stimulated Raman scattering microscopy. *Science* 322(5909):1857–1861.
- Ozeki Y, Dake F, Kajiyama S, Fukui K, Itoh K (2009) Analysis and experimental assessment of the sensitivity of stimulated Raman scattering microscopy. *Opt Express* 17(5):3651–3658.
- Nandakumar P, Kovalev A, Volkmer A (2009) Vibrational imaging based on stimulated Raman scattering microscopy. *New J Phys* 11:033026.
- Saar BG, et al. (2010) Video-rate molecular imaging in vivo with stimulated Raman scattering. *Science* 330(6009):1368–1370.
- Zhang D, Slipchenko MN, Cheng JX (2011) Highly sensitive vibrational imaging by femtosecond pulse stimulated Raman loss. *J Phys Chem Lett* 2(11):1248–1253.
- Wang MC, Min W, Freudiger CW, Ruvkun G, Xie XS (2011) RNAi screening for fat regulatory genes with SRS microscopy. *Nat Methods* 8(2):135–138.
- Zhang X, et al. (2012) Label-free live-cell imaging of nucleic acids using stimulated Raman scattering microscopy. *ChemPhysChem* 13(4):1054–1059.
- Fu D, et al. (2012) Quantitative chemical imaging with multiplex stimulated Raman scattering microscopy. *J Am Chem Soc* 134(8):3623–3626.
- Ozeki Y, et al. (2012) High-speed molecular spectral imaging of tissue with stimulated Raman scattering. *Nat Photonics* 6:845–851.
- Einstein A (1917) On the quantum theory of radiation. *Phys Z* 18:121–128.
- Bloembergen N (1967) The stimulated Raman effect. *Am J Phys* 35(11):989–1023.
- Min W, Freudiger CW, Lu S, Xie XS (2011) Coherent nonlinear optical imaging: Beyond fluorescence microscopy. *Annu Rev Phys Chem* 62:507–530.
- Min W (2011) Label-free optical imaging of nonfluorescent molecules by stimulated radiation. *Curr Opin Chem Biol* 15(6):831–837.
- Okayasu T, Ikeda M, Akimoto K, Sorimachi K (1997) The amino acid composition of mammalian and bacterial cells. *Amino Acids* 13(3–4):379–391.
- Phair RD, Misteli T (2000) High mobility of proteins in the mammalian cell nucleus. *Nature* 404(6778):604–609.
- Andersen JS, et al. (2005) Nucleolar proteome dynamics. *Nature* 433(7021):77–83.
- Boisvert FM, et al. (2012) A quantitative spatial proteomics analysis of proteome turnover in human cells. *Mol Cell Proteomics* 11(3):M111.011429.
- Piez KA, Eagle H (1958) The free amino acid pool of cultured human cells. *J Biol Chem* 231(1):533–545.
- Lechene CP, Luyten Y, McMahon G, Distel DL (2007) Quantitative imaging of nitrogen fixation by individual bacteria within animal cells. *Science* 317(5844):1563–1566.
- Zhang DS, et al. (2012) Multi-isotope imaging mass spectrometry reveals slow protein turnover in hair-cell stereocilia. *Nature* 481(7382):520–524.
- van Manen HJ, Lenferink A, Otto C (2008) Noninvasive imaging of protein metabolic labeling in single human cells using stable isotopes and Raman microscopy. *Anal Chem* 80(24):9576–9582.

Supporting Information

Wei et al. 10.1073/pnas.1303768110

SI Materials and Methods

Stimulated Raman Scattering Microscopy. An integrated laser (picoEMERALD; Applied Physics & Electronics) was used as the light source for both Pump and Stokes beams. Briefly, picoEMERALD provides an output pulse train at 1,064 nm with 7-ps pulse width and 80-MHz repetition rate, which serves as the Stokes beam. The frequency-doubled beam at 532 nm is used to synchronously seed a picosecond optical parametric oscillator to produce a mode-locked pulse train [the idler beam of the optical parametric oscillator (OPO) is blocked with an interferometric filter] with 5- to ~6-ps pulse width. The wavelength of the OPO is tunable from 720 to 990 nm, which serves as the Pump beam. The intensity of the 1,064 nm Stokes beam is modulated by a built-in acousto-optic modulator at 10 MHz driven by a square-wave function generator with a modulation depth of more than 70%. The Pump beam is spatially overlapped with the Stokes beam with a dichroic mirror inside picoEMERALD. The temporal overlap between Pump and Stokes pulse trains is ensured with a built-in delay stage and optimized by the stimulated Raman scattering (SRS) signal of pure dodecane liquid.

Pump and Stokes beams are coupled into an inverted laser-scanning microscope (FV1000MPE; Olympus) optimized for near-IR throughput. A 60 \times water objective (UPlanAPO/IR; 1.2 N.A.; Olympus) with high near-IR transmission is used for all cell imaging. The Pump/Stokes beam size is matched to fill the backaperture of the objective. The forward-going Pump and Stokes beams after passing through the sample are collected in transmission with a high N.A. condenser lens (oil immersion, 1.4 N.A.; Olympus), which is aligned following Kohler illumination. A telescope is then used to image the scanning mirrors onto a large area (10 \times 10 mm) Si photodiode (FDS1010; Thorlabs) to detect beam motion during laser scanning. The photodiode is reversed bias by 64 V from a DC power supply to increase both the saturation threshold and response bandwidth. A high OD bandpass filter (890/220 CARS; Chroma Technology) is used to block the Stokes beam completely and transmit the Pump beam only. The output current of the photodiode is electronically prefiltered by a bandpass filter (BBP-10.7; Mini Circuits) to suppress both the 80-MHz laser pulsing and the low-frequency contribution due to laser scanning cross the scattering sample. It is then fed into a radio frequency lock-in amplifier (SR844; Stanford Research Systems) terminated with 50 Ω to demodulate the stimulated Raman loss signal experienced by the Pump beam. The R-output of the lock-in amplifier is fed back into the analog interface box (FV10-ANALOG) of the microscope. The time constant is set for 20 μ s

(the shortest available with no additional filter applied). The current SRS imaging speed is limited by the shortest time constant available from the lock-in amplifier (SR844). For imaging, 512 \times 512 pixels are acquired for one frame with a 100 μ s of pixel dwell time and 20 μ s of time constant from the lock-in amplifier. Laser powers after 60 \times IR objective used for cell imaging are as follows: 61 mW for modulated Stokes beam; 145 mW for the Pump beam of 2,133 cm^{-1} , 2,000 cm^{-1} , and 1,655 cm^{-1} channels; and 64 mW for Pump beam of 2,950 cm^{-1} and 2,845 cm^{-1} channels.

Sample Materials for SRS Microscopy. Leucine-, lysine-, arginine-deficient DMEM (catalog no. D9443), L-lysine (catalog no. L8662), L-arginine (catalog no. A8094), L-leucine-2,3,3,4,5,5,5',5',5'- d_{10} (catalog no. 492949), and retinoic acid (catalog no. R2625) were obtained from Sigma. Uniformly deuterium-labeled cell free amino acid mix (20 aa) (DLM-6819) was from Cambridge Isotope Laboratories. Homopropargylglycine (Hpg) and Click-iT Hpg Alexa Fluor 488 Imaging Kit (catalog no. C10428) were purchased from Invitrogen.

Deuterium-labeled DMEM (containing either leucine- d_{10} or deuterium-labeled all amino acids) was prepared by adding the appropriate amounts (same final concentration as in the regular DMEM) of leucine- d_{10} together with non-deuterium-labeled regular lysine and arginine stock solutions; or of deuterium-labeled cell free amino acid mix solution, into leucine-, lysine-, arginine-deficient DMEM supplied with 10% (vol/vol) FCS, 100 U/mL penicillin, and 50 $\mu\text{g/mL}$ streptomycin. The deuterium-labeled Neurobasal medium for culturing hippocampal neurons is made by supplying all of the essential nutrients with deuterium-labeled amino acids solution for neurons according to Neurobasal medium recipe (Invitrogen), which is then added with B-27 Serum-Free Supplement.

Fluorescence Microscopy Using Bioorthogonal Noncanonical Amino Acid-Tagging Approach. Cells were incubated with 1 mM Hpg, which is an alkyne-bearing analog of methionine, for 20 h. Then fluorescence labeling was conducted using a Click-iT Imaging Kit according to the manufacturer's procedure. Briefly, cells were fixed with 3.7% formaldehyde for 15 min. Then, cells were washed twice with 3% BSA in PBS, followed by incubation with 0.5% Triton X-100 in PBS for 20 min. After washing, cells were incubated with Click-iT reaction mixture for 30 min. Then, after washing with 3% BSA in PBS four times, fluorescence images were obtained using a Leica TCS SP5 confocal microscope while the cells were immersed in PBS solution.

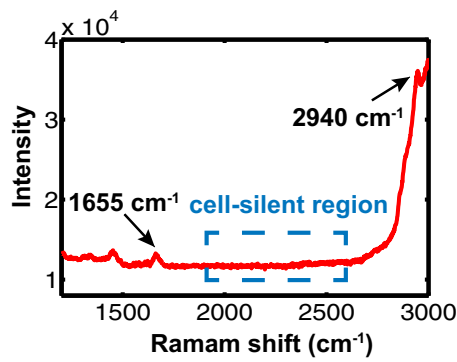


Fig. S1. Spontaneous Raman spectrum from 3,000 cm^{-1} to 1,200 cm^{-1} of HeLa cells growing in a regular medium clearly displays a cell-silent spectral region as highlighted by the blue dashed box. The 2,940 cm^{-1} peak shows the signal of CH_3 stretching mainly from cellular proteins. In addition, the 1,655 cm^{-1} peak shows the amide I stretching signal also primarily from cellular proteins.

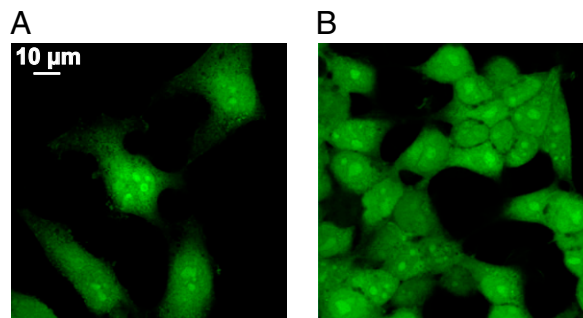


Fig. S2. Fluorescence image of newly synthesized proteins in HeLa and HEK 293T cells using bioorthogonal noncanonical amino acid tagging (BONCAT). By metabolic incorporation of homopropargylglycine (Hpg) followed with fluorescence staining after fixation, permeabilization, and click chemistry using Click-iT Hpg Alexa Fluor 488 Imaging Kit, the newly synthesized proteins are shown in green. The fluorescence images of HeLa cells (A) and HEK293T cells (B) show the maps of newly synthesized proteins in the whole-cell level with nucleoli being highlighted.

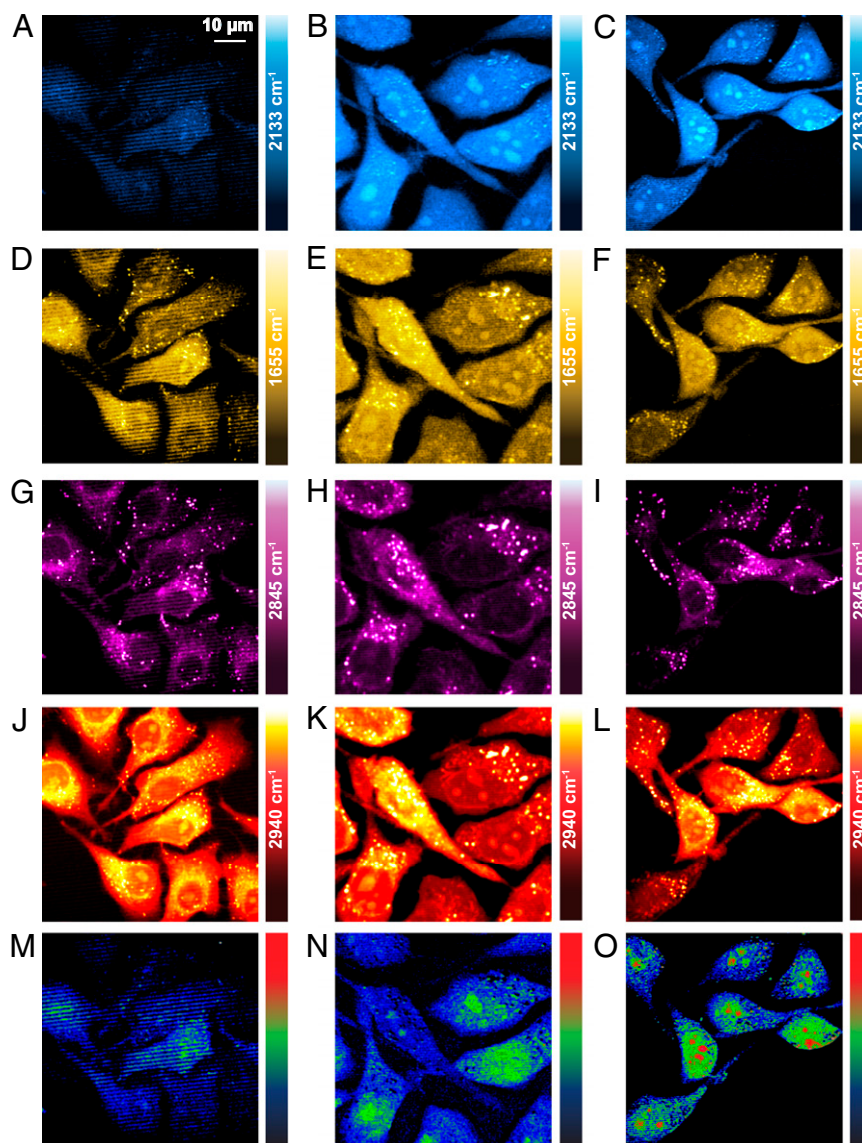


Fig. S3. Multicolor time-dependent SRS imaging of live HeLa cells incubated in deuterium-labeled all-amino acid medium. (A–C) 2,133 cm^{-1} (C–D channel) images of new proteins for cells incubated for 5, 12, and 20 h displaying increasing signals over time. (D–F) The corresponding 1,655 cm^{-1} (amide I channel) images of primarily total proteins show the signals at a steady state. (G–I) 2,845 cm^{-1} (CH_2 channel) images of primarily lipids. (J–L) 2,940 cm^{-1} (CH_3 channel) images of mainly total proteins with minor contribution from lipids. (M–O) Ratio maps between the new proteins (2,133 cm^{-1}) and total proteins (1,655 cm^{-1}) over time, gradually highlighting the nucleoli.

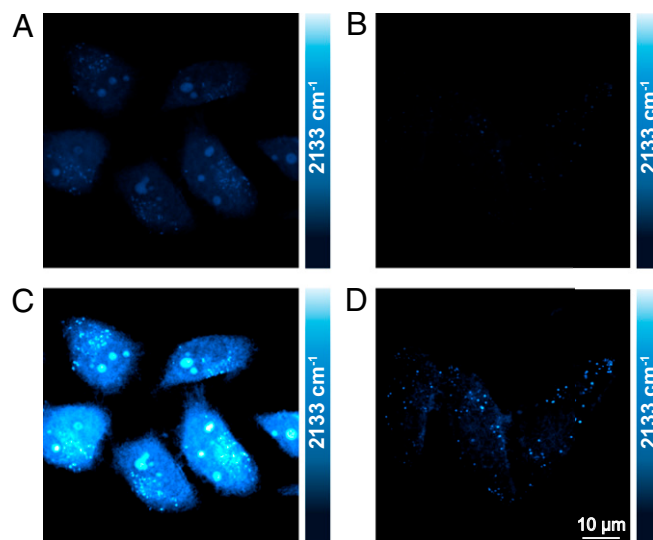


Fig. S4. SRS imaging of drug-induced protein synthesis inhibition effect in live HeLa cells incubated in deuterium-labeled all-amino acid medium. *A* shows the SRS image targeting the $2,133\text{ cm}^{-1}$ of C–D vibration peak for newly synthesized proteins during 5 h of incubation with a deuterium-labeled set of all amino acids. Note that the color scale of this image adapts the same intensity scale as shown in Fig. 4 *A–C* to illustrate the time-dependent signal growth. In contrast, *B* displays the “vanishing” signal when $5\text{ }\mu\text{M}$ anisomycin was coinubated in the medium to block protein synthesis. When the image color scale of both *A* and *B* are amplified by five times, *C* and *D* are the resulting amplified images. *C* shows the same cells but with five times higher brightness (even with partial saturation) than *A*. *D* now starts to exhibit some faint but identifiable image contrast, which is possibly due to the intracellular free amino acids pool (1).

1. Piez KA, Eagle H (1958) The free amino acid pool of cultured human cells. *J Biol Chem* 231(1):533–545.

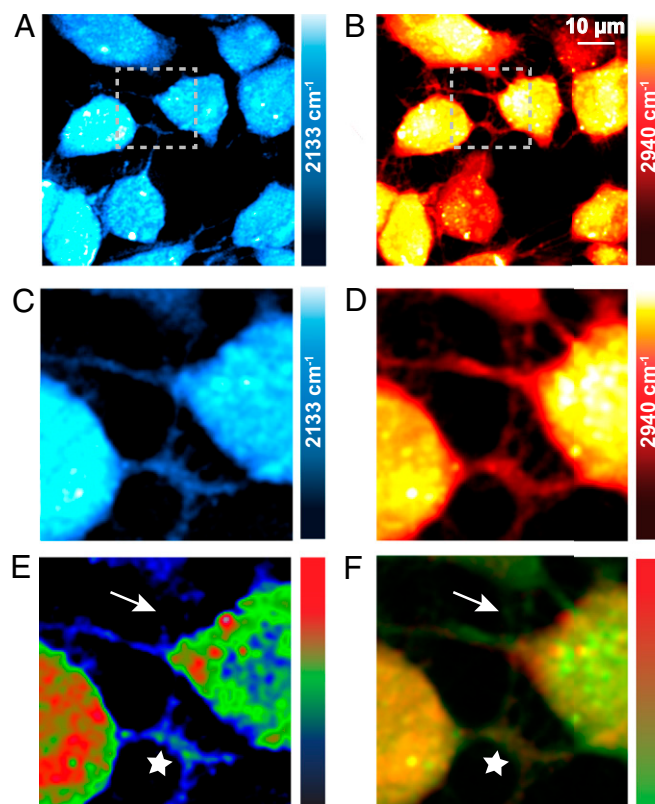


Fig. S5. SRS imaging of newly synthesized proteins in both cell bodies and newly grown neurites of neuron-like differentiable mouse neuroblastoma (N2A) cells. During the cell differentiation process by serum deprivation and $1\ \mu\text{M}$ retinoic acid, a deuterium-labeled set of all amino acids is also supplied for 24 h. (A) SRS images targeting the central $2,133\ \text{cm}^{-1}$ vibrational peak of C–D bond show the newly synthesized proteins. (B) SRS images targeting the $2,940\ \text{cm}^{-1}$ CH_3 show the total proteins. (C and D) Zoomed-in images as indicated in the white dashed squares in A and B. (E) Ratio image between new proteins (C) and total proteins (D). Although the starred neurites show relatively high percentage of new protein, the arrows indicated neurites displaying low new proteins percentage. (F) Merged image between new protein (C) (red channel) and total proteins (D) (green channel). Similarly, the starred regions show obvious new proteins, whereas the arrows indicate regions that have low-level new protein signal.

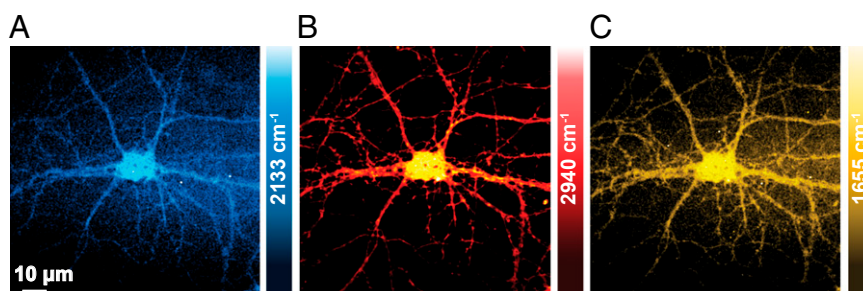


Fig. S6. SRS imaging of newly synthesized proteins in both cell bodies and neurites of live hippocampal neurons growing in Neurobasal medium supplied with deuterium-labeled amino acids for 24 h. (A) SRS image targeting $2,133\ \text{cm}^{-1}$ vibrational peak of C–D bond shows the newly synthesized proteins in both cell bodies and part of the neurites. SRS images at $2,940\ \text{cm}^{-1}$ (B) and $1,655\ \text{cm}^{-1}$ (C) are both attributed mainly to total proteins.